第 28 卷第 10 期
2012 年 10 月

无 机 化 学 学 报
CHINESE JOURNAL OF INORGANIC CHEMISTRY

Vol.28 No.10
2241-2247

简单的溶剂热法制备分层的碲化铋微米结构

谭乃迪[1] 张延林[2] 陈 峰[3] 陈 哲*,[1]

([1]吉林化工学院,吉林 132022)

([2]东北电力大学,吉林 132012)

([3]吉林石化公司有机合成厂,吉林 132021)

摘要:采用简单的溶剂热法制备出高纯度的由纳米片自组装而形成的碲化铋微米结构。在碲化铋的形成中,乙二醇不仅作为溶剂,而且还作为还原剂。研究发现,聚乙烯吡咯烷酮(PVP)和硝酸在碲化铋的形成中起到了很重要的作用。通过 X-射线衍射(XRD)、X-射线光电子能谱(XPS)、扫描电镜(SEM)、透射电镜(TEM)、高分辨透射电镜(HRTEM)、选区电子衍射(SAED)对其进行表征及研究。最后,利用时间演化实验对碲化铋的形成机理进行了探讨。

关键词:碲化铋;分层微米结构;聚乙烯吡咯烷酮;硝酸

中图分类号:O612.5 **文献标识码**:A **文章编号**:1001-4861(2012)10-2241-07

One-Step Solvothermal Synthesis of Hierarchical Bi_2Te_3 Microstructures

TAN Nai-Di[1] ZHANG Yan-Lin[2] CHEN Feng[3] CHEN Zhe*,[1]

([1]*Jilin Institute of Chemical Technology, Jilin, Jilin* 132022, *China*)

([2]*Department of Chemical Engineering, Northeast Dianli University, Jilin, Jilin* 132012, *China*)

([3]*Jinlin Petrochemical Company Organic Synthetic Plants, Jinlin, Jilin* 132021, *China*)

Abstract: High-quality hierarchical microstructures of Bi_2Te_3 self-assembled by nanoplates were prepared via a simple wet chemical method under solvothermal conditions. Ethylene glycol was used not only as a solvent, but also as a reducing agent. The poly(vinyl pyrrolidone)(PVP) and nitric acid played an important role in the construction of the hierarchically self-assembled microstructures. The products were characterized by X-ray diffraction (XRD), X-ray photoelectron spectra (XPS), scanning electron microscopy (SEM), transmission electron microscopy (TEM), high-resolution transmission electron microscopy (HRTEM), and selected area electron diffraction (SAED). A formation mechanism was also proposed based on the result of time-dependent microstructures.

Key words: Bi_2Te_3; hierarchical microstructures; poly(vinyl pyrrolidone)(PVP); nitric acid

In the past few decades, synthesis of micro- and nano-scale inorganic materials have attracted efforts to develop the materials because of their outstanding properties and potential applications correlated with the morphology of the nanomaterials [1-6]. Specifically, hierarchical architecture via self-assembly has become an intensive and hot research topic because of their unique physical and chemical properties and potential applications in optics, electronics, medicine, ceramics, catalysis, and energy/chemical conversions, and their important roles in the systematic research of structure-property relationships in recently years[7-11]. Thus, three-

收稿日期:2012-03-20。收修改稿日期:2012-06-08。

吉林化工学院校级课题资助项目。

*通讯联系人。E-mail:chenzhe0809@yahoo.com.cn

dimensional (3D) hierarchical architectures assembled by nanostructured building blocks such as nanoplates, nanoparticles, nanoribbons, and nanorods, were extensively investigated[12-16]. Up to now, a wide variety of inorganic materials, including metal oxides, sulfides, hydrates, and other minerals, have been prepared with hierarchical structures. For instance, Zhu, et al. [17] reported the synthesis of hierarchical AlOOH nanostructured microspheres by microwave-assisted solvothermal method. Large-scale CeO_2 hierarchical architectures composed of well-aligned nanorods were prepared through hydrothermal method controllably by Chen and co-workers[18]. Up to the present, much advance has been made, but the fabrication of hierarchical 3D architecture is still a big challenge.

The binary chalcogenides of $A^{V}_2B^{VI}_3$(A=As, Sb, Bi; B =S, Se, Te)are a class of important semiconductor materials having applications in thermoelectric, optoelectronic devices, IR spectroscopy, paints, photo-emitting diodes, and microwave switches, etc [19-21]. Bismuth telluride is one of the best thermoelectric materials because they are available for thermoelectric application near room temperature. They are widely used in thermopiles, thermal sensors, and thermoelectric cooler for laser diodes[22-24]. In this regard, much progress has been made in the synthesis of Bi_2Te_3 multifarious morphology, such as Bi_2Te_3 intermetallic compounds with hierarchical nanostructures synthesized via an electrochemical deposition route[25], Bi_2Te_3 plate-like crystals with homogeneous hexagonal morphology synthesized using a microwave assisted wet chemical method [26], and Bi_2Te_3 nanoparticles and nanowires prepared by solvothermal method with $NaBH_4$ as the reductant [27]. Great progress has been achieved in the synthesis approach, however, most of the above investigations also use additional inorganic reducing agents, for example, $NaBH_4$, N_2H_4, and so on. Thus developing convenient and faster synthetic process using inexpensive, environmentally benignant reagents at lower temperature are still important themes.

Herein, we report a solvothermal process to prepare well-defined Bi_2Te_3 nanostructures self-assembled through nanoplates using $Bi(NO)_3$ and Te powder as precursors, and poly(vinyl pyrrolidone) (PVP) as a soft template in ethylene glycol(EG).

1 Experimental

1.1 Materials

All chemicals were used as receieved without further purification. $Bi(NO)_3\cdot 5H_2O$ and PVP (K_{90}) were purchased from Sinopharm Chemical Reagent Co. Ltd.; Te powder was from Jingchun Chemical Reagents Company; Ethylene glycol was from Tianjin Guangfu Chemical Reagents Company; HNO_3 (85wt% solution) was from Beijing Chemical Reagents Company.

1.2 Synthesis

Bi_2Te_3 with different nanostructures were prepared by a simple solvothermal method in the presence of PVP. In a typical synthesis, 3 mmol·L^{-1} $Bi(NO)_3\cdot 5H_2O$ and 9 mmol·L^{-1} PVP (K_{90}) were dissolved in 60 mL ethylene glycol. Then, 4.5 mmol·L^{-1} Te powder, and an appropriate quantity of HNO_3 aqueous solution (5 mol·L^{-1}) were added into the above solution and transferred into an 80 mL Teflon-lined stainless steel autoclave under stirring. The autoclave was maintained at 180 ℃ for 48 h and then cooled to room temperature in air. The resulting solid product was collected and washed with deionized water and ethanol, and finally dried at room temperature for 12 h.

1.3 Characterization

The resulting samples were characterized by Rigaku D/Max2500PC X-ray powder diffraction (XRD) equipped with graphite monochromatized Cu $K\alpha$ radiation (λ=0.154 18 nm) under the following conditions: 30 kV as accelerating voltage; 100 mA as emission current; and the 2θ range of 5°~90° at a scan rate of 4°·min^{-1}. The morphology and dimension of samples were observed by field emission scanning electron microscopy (FE-SEM, JEOL 7500B) and transmission electron microscopy (TEM, H-800). The microstructure of samples was determined using high-resolution transmission electron microscopy (HRTEM) on a JEM-2010 apparatus with an acceleration voltage of 200 kV. X-ray photoelecton spectroscopy (XPS, ESCALAB 250) was used to confirm the oxidation state

of iron.

2 Results and discussion

A typical powder X-ray diffraction (XRD) pattern of the as-synthesized powder formed via template-assisted solvothermal synthesis is shown in Fig.1. All of the diffraction peaks can be readily indexed to pure rhombohedral Bi_2Te_3 crystal (PDF No. 15-0863). No impurities such as Bi_2O_3 and others, which often appear in the Bi_2Te_3 product synthesized by traditional routes, are observed. Furthermore, all diffraction peaks are strong and narrow, indicating the high crystallinity of the Bi_2Te_3 sample.

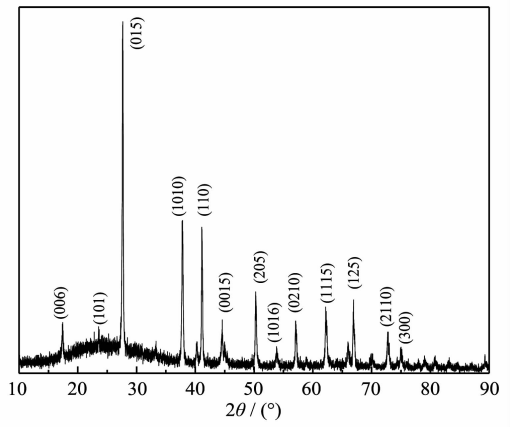

Fig.1 XRD pattern of the sawtooth-like Bi_2Te_3 nanostructures

The X-ray photoelectron spectroscopy (XPS) of the as-prepared sample obtained in the presence of PVP at 180 ℃ was measured to examine the composition of the surface. The wide XPS spectrum in Fig.2a shows that no obvious impurities are detected in the XPS survey spectrum of Bi_2Te_3. It should be noted that only ethylene glycol solvent was used and no other reducing agent was introduced in our system. To prove whether or not ethylene glycol could completely reduce the Te powder to Te^{2-}, XPS was also consulted to unambiguously assign the crystal phase. Fig.2b presents the XPS spectrum of Bi and Te element on the surface of the sample. The two strong peaks at 572.0 eV and 582.3 eV can be attributed to the bonding energies of Te3*d*5/2. The peaks at 575.7 eV and 582.3 eV can be assigned to the bonding energy of Bi3$d_{3/2}$ transition, which perfectly match with the previously published spectra of Bi_2Te_3[28].

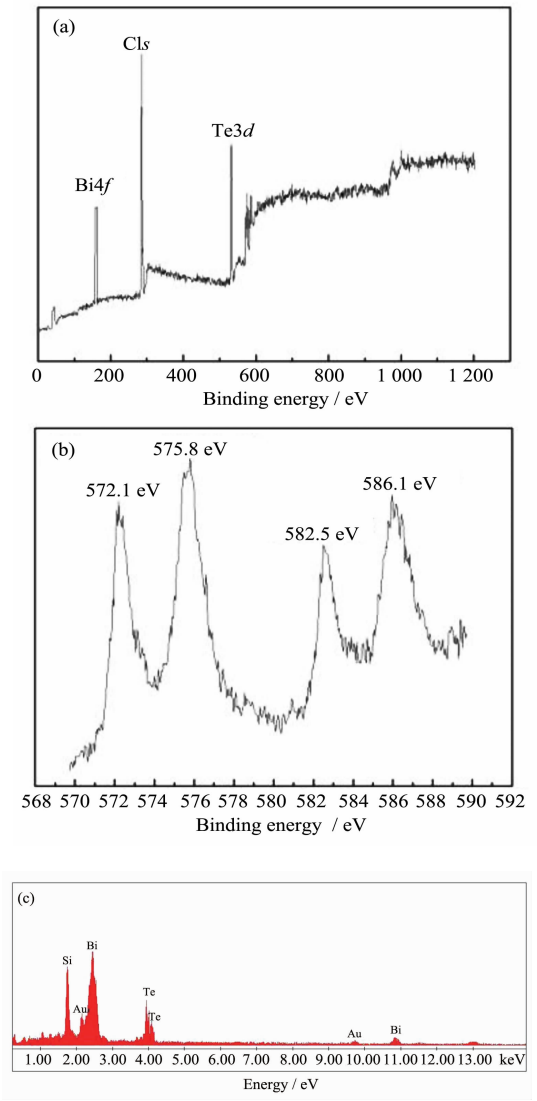

Fig.2 (a) X-ray photoelectron spectra (XPS) of Bi_2Te_3, and (b) Bi3*d* and Te3*d* XPS spectra of the typical as-prepared sample, (c) EDX spectrum of Bi_2Te_3 sample

The composition of the formed Bi_2Te_3 is determined by EDX analysis (Fig.2c) attached to a SEM instrument. The EDS analysis microanalysis clearly demonstrates that only Bi and Te element in the sample with an atomic ratio of Bi / Te is 1:1.51, which is consistent with stoichiometric ratio of Bi_2Te_3. No other impurities are detected in the EDX analysis, such as C, H, and O, indicating the complete disappearance of the surfactants (PVP) during the washing with deionized water and ethanol later process. Si and Au in the EDS spectrum (Fig.2c) originate from the silicon wafer to support and a thin Au layer sputtered on the sample,

respectively. Thus, the XRD, XPS, and EDX spectrum analysis further confirm the high purity for Bi_2Te_3 sample, respectively.

The morphology and size of the as-prepared Bi_2Te_3 sample were characterized by FE-SEM and TEM. A panoramic SEM (Fig.3a) image demonstrates that the product displays sawtooth-like pattern. No other morphologies are observed, indicating a high yield of this sample. As shown by the higher-magnification SEM image in Fig.3b, these sawtooth-like samples are composed of uniform nanoplates with diameters of 30 ~40 nm. The representative TEM images of the Bi_2Te_3 samples obtained at 180 ℃ are shown in Fig.3c and Fig.3d. As indicated by the figures, the as-prepared Bi_2Te_3 samples are consisted of sawtooth rods with diameters of 30~40 nm. Closer observations are shown in Fig.3d, the individual sawtooth rod has an average diameter of 35±10 nm and length of 1 μm, in good accordance with the SEM images. Further structural characterizations for the Bi_2Te_3 samples were carried out by SAED and HRTEM (Fig.3e). A selected area electron diffraction (SAED) pattern (inset in Fig.3e) taken from the edge of sawtooth rods can be indexed as a pure crystalline feature. Fig.3e shows a high-resolution TEM (HRTEM) image taken on individual nanoplate, revealing that each nanoplate is ploy-crystalline and the clear crystal lattices with *d*-spacing of 0.345 nm, which is nearly consistent with the (003) reection plane spacing of the rhombohedral Bi_2Te_3 phase. Thus, all the above-mentioned results clearly demonstrate the successful fabrication of the title material.

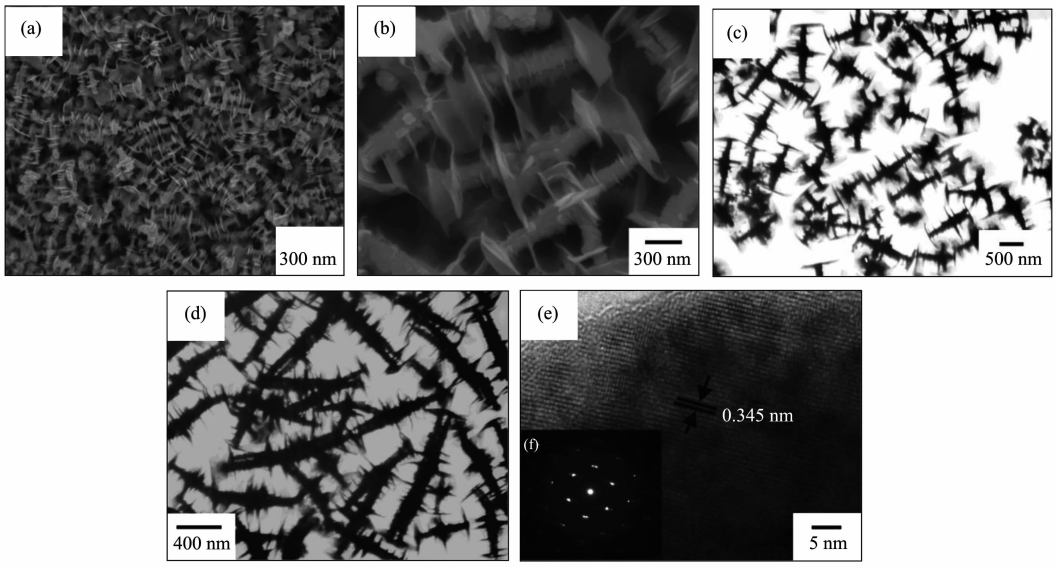

Fig.3 Image of the obtained product: (a) and (b) the FE-SEM image with low and high magnification, respectively (c), and (d) TEM images (e) HRTEM image (f) SAED pattern

The current synthesis strategy provides powerful means to tailor the composition, purity, and assembly of Bi_2Te_3 microstructures as a function of reaction parameters such as concentration of reagents, molar ratio of nitric acid (HNO_3), and addition of PVP. Firstly, to study the influences of nitric acid on the morphology of as-synthesized Bi_2Te_3, controllable experiments were performed by changing reaction parameters. The nitric acid is essential for the development of the sawtooth rod. Fig.4 shows the TEM image of the sample synthesized in the same experimental condition except the volume of nitric acid. Perfect rose-like microflowers with diameters of 1 ~1.5 μm are formed without the addition of nitric acid (Fig.4a). When 2 mL of the above nitric acid aqueous solution is used, it can be clearly seen that the products are comprised of a large number of irregular and nonuniform plates with different sizes and a little of sawtooth rod, as shown in Fig. 4b. With the the nitric acid volume added (3 mL) is increased, the perfect 3D flowerlike nanostructures with well-

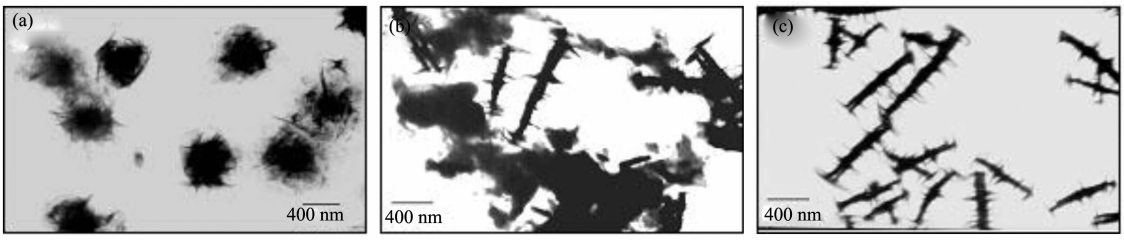

(a) 1 mL; (b) 2 mL; (c) 3 mL

Fig.4　TEM image of the products after adding different amounts of nitric acid

arranged nanoplates are obtained (Fig.4c). Secondly, Fig.5 shows the influence of PVP on the assembly behavior of Bi_2Te_3. The irregular and nonuniform nanoplates with a small size are formed without the used of PVP as shown in Fig.5a. When the PVP usage is increased to 3 mmol·L^{-1} (Fig.5b), both irregular nanoplates and sawtooth rods are obtained. Fig.5c further exhibits the morphologies of the products when 9 mmol·L^{-1} PVP is used, namely the optimum synthesized condition, and a great deal of well-defined sawtooth-like nanostructures self-assembled by nanoplates are observed. Further increase in the concentration of PVP (27 mmol·L^{-1}) leads to the formation of sawtooth-like microstructures with large length and width. Thus, these observations clearly show that the concentration of PVP in the system also has a great effect on the morphology of the products (Fig.5d). Finally, the concentration of reactants is another important influence factor on the morphology of Bi_2Te_3 sample. Fig.6 presents TEM images of Bi_2Te_3 nanostructures obtained with different concentrations of reactants. When 5 mmol·L^{-1} of $Bi(NO_3)_3$ is used, as shown in Fig.6a, a few of nanorods with different diameters are found in the product. When the concentration of initial reagents is increased from 0.5 mmol·L^{-1} to 1 mmol·L^{-1} and other reaction parameters are similar to the product shown in Fig.6b, lots of well-defined dispersed sawtooth-like microstructures are obtained. If only 3 mmol·L^{-1} of $Bi(NO_3)_3$ is used, the resulting sample has irregular morphology (Fig.6c). According to the above results, we can conclude that the sawtooth-like microstructures strongly depend on the concentrations of $Bi(NO_3)_3$ and PVP, molar ratio of nitric acid, respectively.

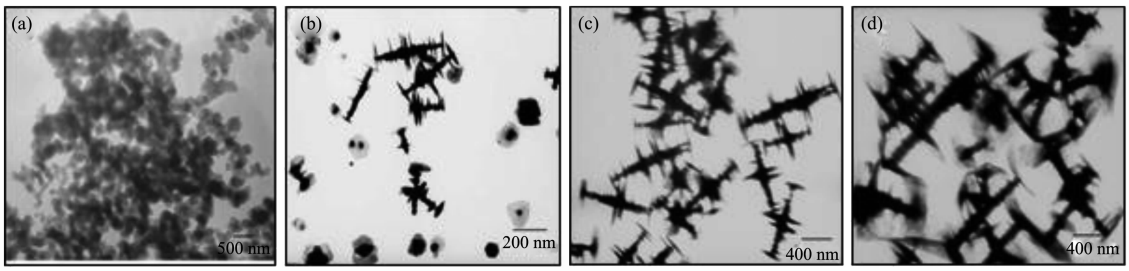

(a) no PVP; (b) 3 mmol·L^{-1}; (c) 9 mmol·L^{-1}; (d) 27 mmol·L^{-1}, respectively

Fig.5　TEM image of the products with different concentrations of PVP

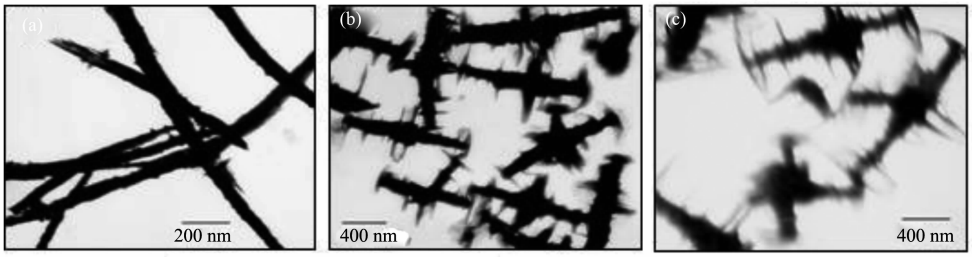

(a) 5 mmol·L^{-1}; (b) 1 mmol·L^{-1}; (c) 3 mmol·L^{-1}, respectively

Fig.6　TEM image of the products with different concentrations of $Bi(NO_3)_3$

To further confirm the formation mechanism of these sawtooth-like microstructures, time-dependent experiments were performed. With a short reaction time (12 h, Fig.7a), the resulted sample are consisted of a great deal of irregular nanoplates and minor amount of nanorods. When the reaction time is up to 24 h, the amount of sawtooth-like morphology are enhanced and nanoplates are decreased comparing with Fig.7a (see Fig.7b). With increasing the reaction time to 36 h, sawtooth rods with different sizes are increased (Fig.7c). It is worth pointing out that nanoplates are far smaller than the one prepared through 24 h. After 36 h of reaction time, nanoplates disappeare, and 3D hierarchical sawtooth-like microstructures with a diameter of 35 nm are obtained (Fig.7d). Although the exact mechanism for the formation of the sawtooth rods microstructures now is not clear, on the basis of the experimental results, a possible interpretation for the formation process of the sawtooth-like structure could be given as follows: at the initial stage of reaction, Te powder may be dissolved in nitric acid[29], and Te^{2-} is produced from the reduction of Te powder by the EG. Then, tiny Bi_2Te_3 crystal nuclei are formed between Bi^{3+} and Te^{2-} through homogeneous nucleation. Further growth of these crystal nuclei results in the formation of nanorods and nanoplates because of their high activity. The initially formed nanoplates begin to assemble in face-to-face growth style and nanorods are located at the center, owning to the interaction with PVP. With time going on, perfect 3D hierarchical sawtooth-like microstructures are formed.

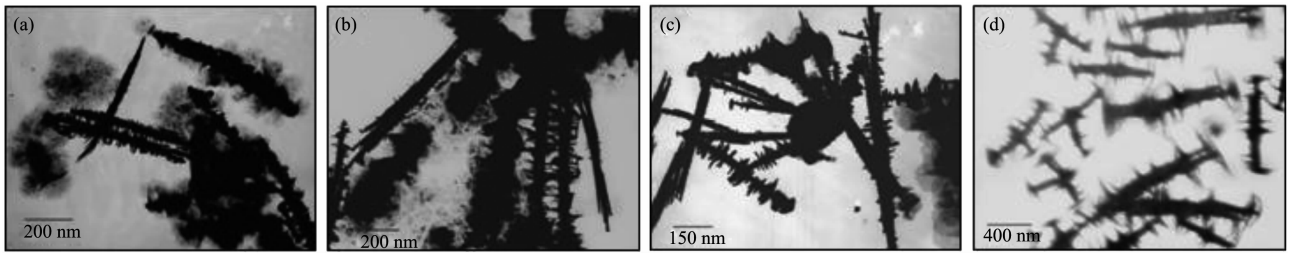

(a) 12 h; (b) 24 h; (c) 36 h; (d) 48 h, respectively

Fig.7 TEM image of the products with different time

3 Conclusions

In summary, high purity Bi_2Te_3 material with hierarchical microstructure self-assembled by nanoplates has been synthesized in mild ethylene glycol hydrothermal system. In the synthesis process, inorganic metal salts are used as raw materials, avoiding from the use of the complicated organic reactions and toxic reagents. Surfactant PVP is introduced as a template for the formation of Bi_2Te_3 hierarchical nanostructure. A formation mechanism is suggested on the basis of the time-dependent experimental results.

References:

[1] Yang H G, Zeng H C. *Angew. Chem., Int. Ed.*, **2004**,**43**: 5930-5933

[2] Shen G Z, Chen D. *J. Am. Chem. Soc.*, **2006**,**128**:11762-11763

[3] Gao P X, Wang Z L. *J. Am. Chem. Soc.*, **2003**,**125**:11299-11305

[4] Hu J, Bando Y, Golberg D, et al. *Adv. Mater.*, **2005**,**17**: 1964-1969

[5] Shi H T, Qi L M, Ma J M. *J. Am. Chem. Soc.*, **2003**,**125**: 3450-3451

[6] Cao M H, Liu T F, Gao S. *Angew. Chem., Int. Ed.*, **2005**,**44**: 4197-4201

[7] Yin Y D, Alivisatos A P. *Nature*, **2005**,**437**:664-670

[8] Wang D L, Lieber C M. *Nat. Mater.*, **2003**,**2**:355-356

[9] Wang Z L. *J. Mater. Chem.*, **2005**,**15**:1021-1024

[10]Burda C, Chen X, El-Sayed M A, et al. *Chem. Rev.*, **2001**, **105**:1025-1102

[11]Xia Y N, Yang P D, Sun Y G. *Adv. Mater.*, **2003**,**15**:353-389

[12]Rhodes K H, Davis S A, Mann S, et al. *Chem. Mater.*, **2000**, **12**:2832-2834

[13]Kim F, Kwan S, Yang P, et al. *J. Am. Chem. Soc.*, **2001**, **123**:4360-4361

[14]Fan X, Meng X M, Lee S T, et al. *Angew. Chem., Int. Ed.*,

2006,**45**:2568-2571

[15]Wu J, Duan F, Xie Y, et al. *J. Phys. Chem. C*, **2007**,**111**: 12866-12871

[16]Zhang X, Ai Z, Jia F, et al. *J. Phys. Chem. C*, **2008**,**112**: 747-753

[17]Zhang L, Zhu Y J. *J. Phys. Chem. C*, **2008**,**112**:16764-16768

[18]Yu R B, Yan L, Zheng P, et al. *J. Phys. Chem. C*, **2008**, **112**:19896-19900

[19]Arivouli D, Gnanam F D, Ramasamy P. J, Mater. Sci. Lett., **1988**,**7**:711-713

[20]Case T W. *Phys. Rev.*, **1917**,**9**:305-310

[21]Tang Q, Zhou W I, Jiang K. *Cryst. Growth Des.*, **2005**,**5**: 147-150

[22]Harman T C, Taylor P J, Walsh M P, et al. *Science*, **2002**,**297**:2229-2232

[23]Chen G, Dresselhaus M S, Dresselhauss G, et al. *Int. Mater. Rev.*, **2003**,**48**:45-66

[24]Harman T C, Taylor P J, Spears D L, et al. *J. Electron. Mater.*, **2000**,**29**:L1-L4

[25]Li G R, Zheng F L, Tong Y X. *Gryst. Growth Des.*, **2008**,**8**: 1226-1232

[26]Fan X A, Yang J Y, Xie Z. *J. Phys. D*: *Appl. Phys.*, **2007**, **40**:5975-5979

[27]Zhao X B, Ji X H, Zhang Y H, et al. *J. Alloys Comp.*, **2004**, **368**:349-352

[28]Kim S H, Kim J J, Suh S W. *J. Ind. Eng. Chem.*, **2010**,**16**: 741-747

[29]Marshall H. *Tellurium*(Ⅳ) *Oxide*: *Tellurium Dioxide* in Harold Simmons Booth eds. *Inorganic Syntheses*: *Vol.*1, **2007**: 143-145, Published Online. DOI: 10.1002/9780470132326